

Direct experimental evidence for anisotropy compensation between Dy³⁺ and Pr³⁺ ions

W. J. Ren,^{a)} J. J. Liu, D. Li, W. Liu, X. G. Zhao, and Z. D. Zhang

Shenyang National Laboratory for Materials Science, Institute of Metal Research and International Centre for Materials Physics, Chinese Academy of Sciences, Shenyang 110016, People's Republic of China

(Received 22 February 2006; accepted 1 August 2006; published online 18 September 2006)

Experimental evidence for the anisotropy compensation between Dy³⁺ and Pr³⁺ ions has been observed directly by performing x-ray diffraction on magnetic-field aligned powders and by evaluating the spin-reorientation temperature and the magnetostriction of Tb_{0.2}Dy_{0.8-x}Pr_x(Fe_{0.9}B_{0.1})_{1.93} alloys. The spin-reorientation temperature decreases with increasing the Pr content. The easy magnetization direction (EMD) at room temperature of the alloys rotates continuously in the (110) plane from ⟨001⟩ for $x=0.18$ to ⟨111⟩ for $x=0.40$, subjected to the anisotropy compensation between Dy³⁺ and Pr³⁺ ions. It is observed that the EMD of some of the alloys lies along nonmajor axes at room temperature. A maximum value of magnetostriction is achieved at $x=0.22$, which is also attributed to the anisotropy compensation. © 2006 American Institute of Physics. [DOI: 10.1063/1.2356109]

The cubic RFe₂ ($R \equiv$ rare earths) compounds usually possess a large magnetostriction as well as a large magnetocrystalline anisotropy at room temperature (RT).^{1,2} A large magnetostriction is useful in transducers and other devices which convert electrical energy to mechanical one. However, a large magnetic anisotropy is a hindrance to the application of the magnetostrictive materials, because then large fields are required to realize a large magnetostriction. In order to lower the magnetocrystalline anisotropy and also to maintain the large magnetostriction, pseudobinary RR'Fe₂ compounds (for example, the well-known Terfenol-D Tb_{0.27}Dy_{0.73}Fe_{1.95}) with the anisotropy compensation were developed by alloying RFe₂ compounds with the same magnetostriction sign but opposite anisotropy signs.¹ But, usually, the Dy_{1-x}Pr_xFe₂ compounds are not taken as a system with the anisotropy compensation because of the same sign of the anisotropy constant K_1 of Dy³⁺ and Pr³⁺ ions.³ Recently, the anisotropy compensation characteristic of Dy_{1-x}Pr_xFe₂ system was proved phenomenologically by taking into account the effects of both the anisotropy constants K_1 and K_2 , and then proved by x-ray crystallography method for Tb_{0.2}Dy_{0.8-x}Pr_x(Fe_{0.9}B_{0.1})_{1.93} alloys, based on the high anisotropic nature of the magnetostriction $\lambda_{111} \gg \lambda_{100}$ in RFe₂ compounds.⁴ That is, the double-split (440) lines of x-ray diffraction (XRD) correspond to the easy magnetization direction (EMD) lying along ⟨111⟩ axes, while a sharp single peak with no observable split-up (440) line corresponds to the ⟨100⟩ EMD.^{1,4} The composition dependence of the magnetocrystalline anisotropy is minimized, when the EMD changes from ⟨100⟩ to ⟨111⟩ axes or reversely. However, if λ_{111} were not large enough in the case of the ⟨111⟩ EMD, the double-split XRD (440) lines would overlap heavily, which might be mistaken as the ⟨100⟩ EMD. Another shortcoming of this x-ray crystallography method was to assume for all the cases that EMD lies along ⟨100⟩ or ⟨111⟩, without considering the cases of ⟨110⟩ and the nonmajor axes. These indicated that the proof of the existence of the anisotropy compensation in Ref. 4 was not very sufficient. In this letter,

the EMD of the Tb_{0.2}Dy_{0.8-x}Pr_x(Fe_{0.9}B_{0.1})_{1.93} ($0 \leq x \leq 0.4$) alloys was straightforwardly determined by performing XRD on powders aligned at a magnetic field. The magnetocrystalline anisotropy at RT of the alloys was evaluated by measuring the spin-reorientation temperature T_{SR} and also the field dependence of the magnetostriction. By these methods, experimental evidence for the anisotropy compensation between Dy³⁺ and Pr³⁺ ions at RT was directly observed and an anisotropy compensation point was accurately obtained. The existence of the anisotropy compensation between Dy³⁺ and Pr³⁺ ions was sufficiently proved experimentally. Furthermore, it was observed that the EMD of some of the alloys lies along nonmajor axes at RT.

All polycrystalline samples of Tb_{0.2}Dy_{0.8-x}Pr_x(Fe_{0.9}B_{0.1})_{1.93} alloys with $x=0, 0.10, 0.14, 0.18, 0.22, 0.26, 0.30, 0.34, 0.37,$ and 0.40 were prepared by arc melting the appropriate constituent metals in a high purity argon atmosphere. The purities of the constituents are 99.9% for Tb, Dy, Pr, and B, and 99.8% for Fe. The ingots were homogenized at 973 K for seven days in a high purity argon atmosphere. Magnetization curves at RT were measured by a superconducting quantum interference device (SQUID) magnetometer at fields up to 50 kOe. The temperature dependences of ac initial susceptibility were measured using the SQUID to determine the T_{SR} . In order to study the EMD of the Laves phases, aligned samples were prepared by mixing fine powders of the samples with a resin-doped epoxy solution at RT and then putting the mixture into a mold with a circular cavity of $\phi 10 \times 2$ mm². Then an external magnetic field of 15 kOe was applied for 8 h when the epoxy resin solidified. XRD was implemented on the surface of Tb_{0.2}Dy_{0.8-x}Pr_x(Fe_{0.9}B_{0.1})_{1.93}/epoxy at RT with Cu $K\alpha$ radiation in a Rigaku D/max-2500pc diffractometer equipped with a graphite monochromator. The magnetostriction at RT was measured either parallel or perpendicular to the applied field using a standard strain gauge technique.

The magnetization curves for Tb_{0.2}Dy_{0.8-x}Pr_x(Fe_{0.9}B_{0.1})_{1.93} alloys at RT (295 K) was shown in Fig. 1. The dependence of the saturation magnetization M_s on the nominal Pr content x was plotted in the

^{a)}Electronic mail: wjren@imr.ac.cn

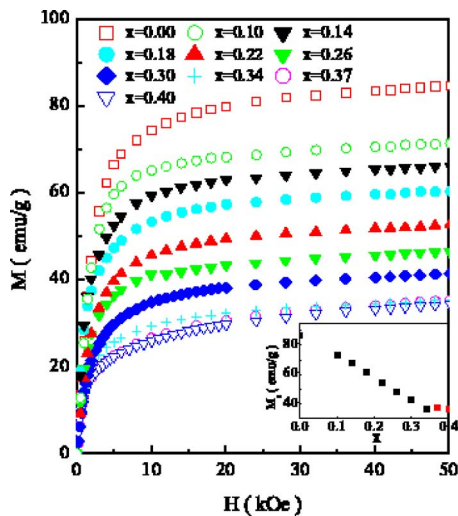


FIG. 1. (Color online) Magnetization curves and saturation magnetization M_s at 295 K for $\text{Tb}_{0.2}\text{Dy}_{0.8-x}\text{Pr}_x(\text{Fe}_{0.9}\text{B}_{0.1})_{1.93}$ alloys.

inset of Fig. 1. M_s decreases linearly with increasing the Pr content as $0 \leq x \leq 0.34$, since the magnetic moment of Pr (or Dy) aligns parallel (or antiparallel) to that of Fe. M_s does not change markedly when $x > 0.34$, suggesting that the Pr content in Laves phase is not equal to the nominal composition of the alloy anymore. It is consistent with the previous result that the increase of the lattice parameter becomes less pronounced when $x > 0.4$, because of the appearance of the impurity phase.⁴

The temperature dependence of the ac initial susceptibility for $\text{Tb}_{0.2}\text{Dy}_{0.8-x}\text{Pr}_x(\text{Fe}_{0.9}\text{B}_{0.1})_{1.93}$ alloys was represented in Fig. 2. The anomaly at about 10 K is attributed to the Curie temperature T_C (8.7 K) of the small amount of unreacted free Pr with a cubic structure.^{5,6} The anomaly at about 80 K is consistent with the T_{SR} of the unreacted free Dy. The existence of free Dy can be proved also by the XRD pattern of the aligned powders (Fig. 3). The Néel temperature of Dy is 179 K, which should not influence the discussion thereafter on the spin-reorientation transition (SRT) at high temperatures. An obvious increment can be observed in every

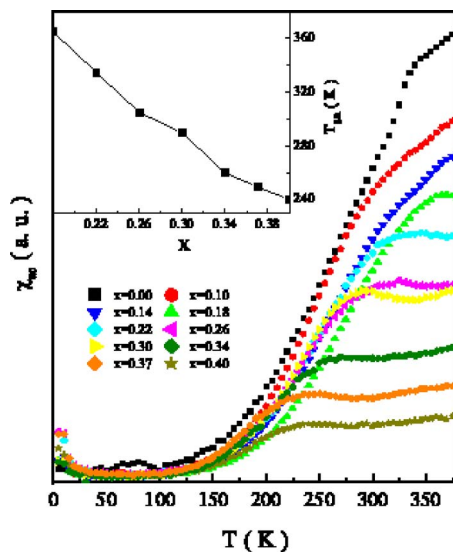


FIG. 2. (Color online) Temperature dependence of ac susceptibility χ_{ac} and composition dependence of the spin-reorientation temperature T_{SR} for $\text{Tb}_{0.2}\text{Dy}_{0.8-x}\text{Pr}_x(\text{Fe}_{0.9}\text{B}_{0.1})_{1.93}$ alloys.

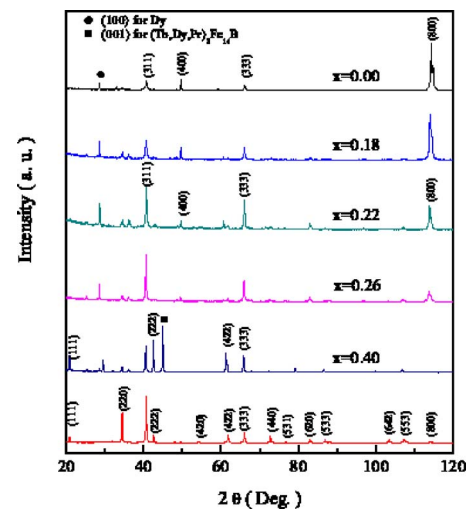


FIG. 3. (Color online) XRD patterns for aligned $\text{Tb}_{0.2}\text{Dy}_{0.8-x}\text{Pr}_x(\text{Fe}_{0.9}\text{B}_{0.1})_{1.93}$ particles at room temperature.

$\chi_{\text{ac}}-T$ curve above 150 K, corresponding to the onset of the SRT of the $R\text{Fe}_2$ -type phase. Below T_{SR} , $R\text{Fe}_2$ is a collinear ferrimagnet because the moment of Dy or Tb aligns antiparallel to that of Fe. According to the two-sublattice model,^{7,8} the moment of Dy or Tb rotates nonsynchronously with that of Fe during the SRT, resulting in a noncollinear alignment between the moments of rare earth and Fe. When the transition accomplishes, $R\text{Fe}_2$ becomes a collinear ferrimagnet again. Composition dependence of T_{SR} for $\text{Tb}_{0.2}\text{Dy}_{0.8-x}\text{Pr}_x(\text{Fe}_{0.9}\text{B}_{0.1})_{1.93}$ alloys ($0.18 \leq x \leq 0.40$) was shown in the inset of Fig. 2. T_{SR} decreases from 365 K across RT to 240 K as x is increased from 0.18 to 0.40. The EMD of the Dy-rich alloys with $T_{\text{SR}} > \text{RT}$ prefers to lie along the $\langle 100 \rangle$ axis at RT, whereas that of the Dy-poor alloys with $T_{\text{SR}} < \text{RT}$ favors to lie along the $\langle 111 \rangle$ axis at RT. This originates from different anisotropies of DyFe_2 and PrFe_2 , whose EMD lie along $\langle 100 \rangle$ and $\langle 111 \rangle$ axes at RT, respectively.^{9,10} The alloys for $0 \leq x < 0.18$ may have a higher T_{SR} over 380 K (or no spin reorientation occurs at the whole temperature range up to Curie temperature).

The XRD patterns at RT for aligned $\text{Tb}_{0.2}\text{Dy}_{0.8-x}\text{Pr}_x(\text{Fe}_{0.9}\text{B}_{0.1})_{1.93}$ powders were represented in Fig. 3. The bottom curve with (hkl) indices is for random $\text{Tb}_{0.2}\text{Dy}_{0.62}\text{Pr}_{0.18}(\text{Fe}_{0.9}\text{B}_{0.1})_{1.93}$ powders. The (800) line of the random powders is very weak, but that of the aligned $\text{Tb}_{0.2}\text{Dy}_{0.8-x}\text{Pr}_x(\text{Fe}_{0.9}\text{B}_{0.1})_{1.93}$ ($0 \leq x < 0.18$) alloys is the strongest peak in their patterns, indicating the $\langle 100 \rangle$ EMD. The intensity of (400) and (800) peaks weakens, while that of (111)-type peaks strengthens with increasing the Pr content. The intensity of (311), (333), and (800) peaks is comparable for the alloy with $x=0.22$, suggesting that it has a very small anisotropy at RT. For the alloys with $0.26 \leq x \leq 0.40$, the (400) and (800) peaks become very weak, indicating that the EMD of these alloys deviates from $\langle 100 \rangle$ axis. It can be said that the EMD for $\text{Tb}_{0.2}\text{Dy}_{0.54}\text{Pr}_{0.26}(\text{Fe}_{0.9}\text{B}_{0.1})_{1.93}$ alloy lies along the nonmajor axis $\langle 113 \rangle$ direction. Atzmony *et al.* investigated the spin-orientation diagrams and magnetic anisotropy of the cubic Laves compounds by using a phenomenological calculation and Mössbauer effect method.^{10,11} Nonmajor axes of the easy magnetization were observed in some pseudobinary $R\text{Fe}_2$ compounds, usually at low temperatures, which was explained by taking into ac-

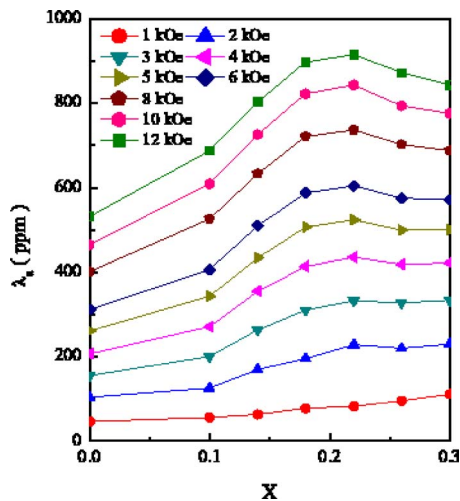


FIG. 4. (Color online) Magnetostriction $\lambda_a = \lambda_{\parallel} - \lambda_{\perp}$ for $\text{Tb}_{0.2}\text{Dy}_{0.8-x}\text{Pr}_x(\text{Fe}_{0.9}\text{B}_{0.1})_{1.93}$ alloys at different applied magnetic fields.

count the action of the anisotropy constant K_3 , besides K_1 and K_2 .¹¹ In fact, in the pseudobinary Laves compounds with the anisotropy compensation, the action of K_3 cannot be ignored in the temperature region where the SRT occurs, because K_1 and K_2 of the alloys are small due to the compensation. This results in the appearance of the nonmajor axes of EMD even at RT. The EMD at RT was found to lie along the $\langle 112 \rangle$ direction in (110) Terfenol-D thin film.¹² The EMD of nonmajor axes appeared in SmFe_2 and $\text{Ho}_x\text{Tb}_{1-x}\text{Fe}_2$, in which the EMD rotated continuously with increasing/decreasing temperature during the SRT.^{13–15} In the SRT region of SmFe_2 , the EMD rotated continuously from $\langle 110 \rangle$ at 180 K toward $\langle 111 \rangle$ at 220 K.¹³ The EMD of the single crystal $\text{Ho}_{0.865}\text{Tb}_{0.135}\text{Fe}_2$ lie along $\langle 110 \rangle$ at 300 K. It rotated continuously from $\langle 110 \rangle$ to $\langle 100 \rangle$ in the (001) plane as the temperature was lowered, then returned back to $\langle 110 \rangle$ again at lower temperatures.¹⁵ In Fig. 4, when $x=0.4$, the (006) peak of $\text{Nd}_2\text{Fe}_{14}\text{B}$ -type phase becomes very strong although it was hard to observe from its unaligned powder XRD pattern.⁴ Except for this peak, the strongest one is the (222) peak of RFe_2 compound, indicating that the EMD lies along $\langle 111 \rangle$ axis. It can be summarized that the EMD at RT of the alloys rotates continuously from $\langle 100 \rangle$ for $x=0.18$ to $\langle 111 \rangle$ for $x=0.40$ in the (110) plane, due to the anisotropy compensation between Dy^{3+} and Pr^{3+} ions.

The composition dependence of magnetostriction $\lambda_a = \lambda_{\parallel} - \lambda_{\perp}$ at different magnetic fields for $\text{Tb}_{0.2}\text{Dy}_{0.8-x}\text{Pr}_x(\text{Fe}_{0.9}\text{B}_{0.1})_{1.93}$ alloys was shown in Fig. 4. Usually, λ_a of magnetostrictive alloys with a single Laves phase is predominately determined by the magnetostriction coefficients λ_{111} and λ_{100} and the magnetocrystalline anisotropy, if the influence of the microstructure is not taken into account temporarily. It has been found that λ_{111} of the alloys increases with increasing x . Moreover, $\lambda_{111} \gg \lambda_{100}$, and thus the action of λ_{100} can be neglected. It can be concluded from the analysis above that λ_a , exhibiting a maximum value at $x=0.22$, should be attributed to reach the minimum of magnetocrystalline anisotropy. It is consistent with the XRD result for aligned powders in Fig. 3, and therefore, this alloy should have a very small anisotropy at RT.

This work has been supported by the National Natural Science Foundation of China under Grant Nos. 50501021 and 50332020.

- ¹A. E. Clark, in *Ferromagnetic Materials*, edited by E. P. Wohlfarth (North-Holland, Amsterdam, 1980), Vol. 1, p. 531.
- ²N. C. Koon, C. M. Williams, and B. N. Das, *J. Magn. Magn. Mater.* **100**, 173 (1991).
- ³A. E. Clark, H. Belson, and N. Tamagawa, *Phys. Lett.* **42A**, 160 (1972).
- ⁴W. J. Ren, Z. D. Zhang, X. P. Song, X. G. Zhao, and X. M. Jin, *Appl. Phys. Lett.* **82**, 2664 (2003).
- ⁵K. A. McEwen, in *Handbook on the Physics and Chemistry of Rare Earth*, edited by K. A. Gschneidner, Jr. and L. R. Eyring (North-Holland, Amsterdam, 1978), Vol. 1, p. 411.
- ⁶W. J. Ren, Z. D. Zhang, X. G. Zhao, W. Liu, and D. Y. Geng, *Appl. Phys. Lett.* **84**, 562 (2004).
- ⁷K. H. J. Buschow, in *Ferromagnetic Materials*, edited by E. P. Wohlfarth (North-Holland, Amsterdam, 1980), Vol. 1, p. 297.
- ⁸Z. D. Zhang, T. Zhao, P. F. de Châtel, and F. R. de Boer, *J. Magn. Magn. Mater.* **147**, 74 (1995).
- ⁹M. Shimotomai, H. Miyake, and M. Doyama, *J. Phys. F: Met. Phys.* **10**, 707 (1980).
- ¹⁰U. Atzmony, M. P. Dariel, E. R. Bauminger, D. Lebenbaum, I. Nowik, and S. Ofer, *Phys. Rev. B* **7**, 4220 (1973).
- ¹¹U. Atzmony and M. P. Dariel, *Phys. Rev. B* **13**, 4006 (1976).
- ¹²C. de la Fuente, J. I. Arnaudas, L. Benito, M. Ciria, A. del Moral, C. Dufour, and K. Dumesnil, *J. Phys.: Condens. Matter* **16**, 2959 (2004).
- ¹³V. S. Gaviko, A. V. Korolyov, and N. V. Mushnikov, *J. Magn. Magn. Mater.* **157–158**, 659 (1996).
- ¹⁴G. Dublon, U. Atzmony, M. P. Dariel, and H. Shaked, *Phys. Rev. B* **12**, 4628 (1975).
- ¹⁵C. M. Williams and N. C. Koon, *Solid State Commun.* **27**, 81 (1978).